

# **INFLUENCE OF HETEROGENEITY, WETTABILITY AND COREFLOOD DESIGN ON RELATIVE PERMEABILITY CURVES**

G. HAMON (ELF EXPLORATION PRODUCTION), C. ROY (ENSEEIH)

## **ABSTRACT**

This paper focuses on the effect of small-scale heterogeneity on the laboratory determination of relative permeability curves. Both the experimental characterisation and the influence of heterogeneity on numerical interpretation of corefloods are addressed. The combined effects of small-scale heterogeneity, flow direction and wettability are studied using numerical experiments. Along bedding (i.e. “horizontal plugs”) and across bedding (i.e. “vertical plugs”) waterfloods are simulated using very finely gridded, two dimensional models and input relative permeabilities ( $K_r$ ). Both steady-state and unsteady-state flows are simulated. Output water and oil production, differential pressure as well as local saturation profiles are obtained. Then these results are used as input for determination of relative permeability curves, using inversion techniques. The main conclusions of this study are:

1. Detailed and reliable characterisation of small-scale heterogeneity can be routinely obtained on vertical consolidated cores. Three dimensional imaging techniques or tracer tests must be applied to horizontal consolidated cores to estimate the permeability of streaks parallel to the flow direction. Simplified and approximate estimates of permeability maps can be obtained on unconsolidated cores using inversion techniques.
2. Unsteady-state flow is very sensitive to along-axis heterogeneity and must be disregarded in heterogeneous “horizontal” plugs. In these samples, steady-state flow is more robust but does not reproduce the true relative permeability curves.
3. Unsteady-state or steady-state flows are almost indifferent to along-axis heterogeneity when capillary forces are negligible.
4. When negative capillary forces become significant, true  $K_r$  curves can be extracted from unsteady-state flows in heterogeneous “vertical” plugs provided that one dimensional (1D) permeability and saturation profiles are available.

## **INTRODUCTION**

Most of the methods of interpretation of coreflood experiments assume that the sample is homogeneous. This is particularly true for the analytical approaches, such as JBN (Johnson, et al., 1958) or Jones and Roszelle (1978). Although small-scale heterogeneity can be incorporated in history-matches of experimental corefloods, this is not routinely done, despite the fact that the effects of small-scale heterogeneities on coreflood behaviour have been demonstrated in the literature. Corey (1956) points out that the interplay between the layout of small-scale heterogeneity and the flow direction might generate large errors in

the determination of relative permeability curves. Huppler (1969) proposed a method of building a composite core in order to minimise the effect of permeability differences between plugs. Hamon (1988) also illustrates by numerical simulation the large variations in oil recovery due to the sequence of permeability zones along an oil-wet, across-bedding core sample. Sylte (1998) reached the same conclusions regarding the oilflood performance of a composite core. Kortekaas (1985) concludes that oil is left behind in high permeability zones when flow crosses beddings for water-wet situations. Corbett (1992) reached similar conclusions. He also highlights the fact that the sensitivity of oil recovery to the flooding rate is different when two-phase flows occur along or across bedding. Huang (1994) shows CT-scan saturation maps and confirms previous findings by Kortekaas. Comparison with CT-scans results obtained after an along bedding waterflood: Huang (1995a). shows very large differences in the distribution of saturation within the core but similar final recoveries. Hornarpour (1995) claims that relative permeability curves obtained for along-bedding and across-bedding flow are different. However, a close inspection of the experimental results shows only minor discrepancies. Huang (1995b) shows CT-scan saturation maps in a heterogeneous-wet sample. Oil is trapped in the low permeability layers for intermediate-wet rock whereas it was trapped in the high permeability layers in the water-wet case. Nordtvedt (1999) simulated a steady-state waterflood on a composite core and concluded that reliable Kr curves can be obtained, provided that local permeabilities are known and incorporated in the interpretation. These studies suggest that the determination of relative permeability may be sensitive to small-scale heterogeneity if not properly taken into account.

In the first part of this paper, we will review some experimental methods used to demonstrate and measure local values of permeability and porosity within a reservoir core. The second part is focused on the interplay between the layout of small scale heterogeneities within the core on one hand and the flooding technique on the other hand and their consequences with respect to determination of relative permeability curves. Finally, we will illustrate the benefits of incorporating local saturation profiles in the process of determining relative permeability curves for heterogeneous samples.

## **EVIDENCE OF SMALL-SCALE HETEROGENEITY**

3D computed tomography (CT) density is routinely performed to select the most homogeneous, but representative samples used for core flooding tests. However, check of homogeneity often hinges only on visual inspection of CT scans and is mainly used to discard disturbed or heterogeneous samples. In most cases, core quality is finally addressed using other types of measurements, which may differ according to the core consolidation or orientation:

### Across-bedding samples:

1. 1D x-ray or gamma-ray profiles on dry samples are often not conclusive. 1D x-ray or gamma-ray profiles on both dry and saturated samples often highlight significant

porosity variations. This technique is widely used as 1D x-ray or gamma-ray are often available. However, this technique has some drawbacks:

- An independent relationship between porosity and permeability must be available to translate porosity variations into permeability variations. This type of relationship is often available on consolidated cores, but not for unconsolidated reservoirs.
  - Very thin laminae are usually very difficult to resolve,
  - 1D beams can erroneously average porosity variations when beddings are not perpendicular to the core axis.
2. Closely spaced minipermeameter measurements are the preferred technique. This technique directly captures permeability variations at small-scale as illustrated by Figure 1, and is usually fully-automated and thus fast and cheap. Surface results might be transferred to the whole core using different methods, including CT-scans. Among the main drawbacks are:
    - Probe permeameter does not work on unconsolidated cores.
    - Very thin laminae might not be resolved.
    - 3D permeability maps might be difficult to extrapolate in vuggy carbonate cores (Dauba, 1998).
  3. Differential pressure across the sample during a drainage coreflood. The pre-breakthrough differential pressure during a viscous oil flood is often a very good marker of permeability differences along the sample. This method is particularly useful for unconsolidated samples as permeability zones are identified once the sample has been mounted in the core holder and loaded back to in-situ stress.
  4. 1D x-ray or gamma-ray profiles prior to the start and during the waterflood test often show saturation gradients and therefore demonstrate heterogeneities which might not have been detected previously, typically very thin laminae or permeability gradients on unconsolidated cores. Corresponding  $S_w$  profiles can easily be compared with any type of 1D numerical simulation.

#### Along-bedding samples:

None of the above-mentioned techniques is able to demonstrate and characterise permeability variations parallel to the core axis on cylindrical reservoir cores.

1. 1D x-ray or gamma-ray profiles on dry or saturated cores erroneously average porosity variations.
2. Probe permeametry would only provide evidence of sample-spanning streaks in some cases.
3. 1D x-ray or gamma-ray profiles during the waterflood test also average between zones and will show very dispersed flow resulting from thief layers, but corresponding  $S_w$  profiles are difficult to incorporate into any type of interpretation.
4. A brine/brine tracer test is the only cheap, fast method to demonstrate along-bedding heterogeneity, but it is far from being systematically used. Inversion of miscible flow effluent curves in combination with oversimplified geometry from CT-scans has been recently proposed to assess the contrast in permeability between zones for parallel flow (Dauba,1999). This method works for all types of samples but is particularly useful for

unconsolidated samples as permeability zones are identified once the sample has been mounted in the core holder and loaded back to in-situ stress

More sophisticated methods have been presented, such as inversion of CT-scan concentration profiles during a miscible flow or local saturation profiles during two-phase flow but they all require a CT-scanner and are rarely used. External relationship between porosity and permeability must be available to translate porosity variations into permeability variations. This short review of experimental methods does show that:

- Several experimental techniques are currently and widely available to demonstrate and characterise small-scale heterogeneity on across-bedding samples prior and during corefloods experiments.
- Very few experimental techniques are currently and widely available to demonstrate and characterise small-scale heterogeneity on along-bedding samples. Using a CT-scan before and during a coreflood is the only way to monitor the consequences of possible small-scale heterogeneity on two-phase behaviour.

It is our experience that ideal, homogeneous samples do not exist. For some reservoirs unfortunately, only very heterogeneous samples are available, as shown by Figure 2. On the other hand, it is clear that it is harder to detect small-scale heterogeneities in samples cut along bedding than those cut across bedding. This probably explains why small “horizontal” plugs are very often considered to be homogeneous without experimental confirmation. In the same way, it is hard to get reliable  $S_w$  profiles during corefloods on samples cut along the bedding as only 1D beams are widely available and this method would smear the individual  $S_w$  profiles in each layer.

## **INTERPLAY BETWEEN SMALL SCALE HETEROGENEITIES AND THE FLOODING TECHNIQUE**

In this section, we study the interplay between the layout of small-scale heterogeneities within the core on one hand and the flooding technique on the other hand and their consequences for the determination of relative permeability curves.

### **Sequence of simulations:**

Each run represents the combined effect of a core flood technique: unsteady-state (USS) versus steady-state (SS) and a typical 3D layout of small-scale heterogeneities. Along-bedding (i.e “horizontal plugs”) and across-bedding (i.e “vertical plugs”) waterfloods are simulated. For each case, 3 steps are reproduced to mimic the interpretation of core floods when small-scale heterogeneity is not accounted for:

1. Numerical simulation of a core waterflood on a heterogeneous sample:
  - Porosity, permeability: the sample is finely gridded. Permeability layout is explicitly represented. Grid refinement is used at each interface between permeability zones with different permeabilities, including inlet and outlet faces. Porosity is assumed to

be constant. One dimensional grids are used when isoperms are perpendicular to the core axis whereas 2D grids are used when isoperms are parallel to the core axis.

- Relative permeability curves: Input curves  $Krwo(Sw)_{input}, Krow(Sw)_{input}$  are assumed to be the same, whatever the permeability.
  - Waterflood capillary pressure curves: are dependent on the cell permeability. Boundary conditions at outlets are explicitly taken into account
  - A multi-rate core waterflood is simulated to decipher the respective effects of relative permeability and capillary pressure curves. Simulation results are water  $Q_w(t)$  and oil production  $Q_o(t)$  versus time as well as differential pressure across the sample  $Dp(t)$ . Local saturations are also available versus time:  $Sw(x, z, t)$ . Average remaining oil saturation:  $Sorw_{output}$  can be calculated at completion of the test as well as the maximum water relative permeability curve:  $Krwo(Sorw_{output})$ .
2. Pseudo relative permeability curves :  $Krwo(Sw)_{output}, Krow(Sw)_{output}$  :
- $Q_w(t), Q_o(t), Dp(t), Sw(x, z, t)$  are now considered as the “experimental observations” obtained during the waterflood on a homogeneous core whose single phase permeability is the average of local values used during the previous step (arithmetic or harmonic). Corresponding relative permeability curves are obtained from these “experimental observations” using inversion techniques. Inversion is constrained by “experimental” end points:  $Sorw_{output}$  and  $Krwo(Sorw_{output})$ . This step mimics routine interpretation schemes, when small-scale heterogeneity has not been checked, or quantified, or accounted for in the numerical simulation. Details about the inversion method used in this paper are reported in Fincham and Gouth (2000).
3. Comparison between true relative permeabilities:  $Krwo(Sw)_{input}, Krow(Sw)_{input}$  and pseudo relative permeabilities :  $Krwo(Sw)_{output}, Krow(Sw)_{output}$  .

This comparison will illustrate :

- The bias in relative permeabilities when small scale heterogeneity is ignored,
- Relationship between bias in relative permeability determinations and 3D layout of local permeabilities
- Relationship between bias in relative permeability determination and flood technique

### **Simulation results:**

Only  $Q_w(t), Q_o(t)$  and  $Dp(t)$  are considered as the “experimental observations” for the inversion process. Capillary pressure is negligible. Several cases were studied:

#### USS flood, along-bedding flow, negligible capillary pressure

Figure 3 compares  $Krwo(Sw)_{output}, Krow(Sw)_{output}$  with  $Krwo(Sw)_{input}, Krow(Sw)_{input}$  . Inversion of experimental observations also results in error bars for each node of

$Krwo(Sw)_{output}$ ,  $Krow(Sw)_{output}$ . Use of error bars helps to show whether input and output curves are significantly different. Figure 4 illustrates the effect of the fraction of the high permeability layer. Both  $Krwo(Sw)_{output}$ ,  $Krow(Sw)_{output}$  are very different from  $Krwo(Sw)_{input}$ ,  $Krow(Sw)_{input}$ . Even a small fraction of the high permeability layer results in a large distortion of  $Krwo(Sw)_{output}$  at low water saturations. Increasing fractions of the high permeability layer result in increasingly large bias in  $Krwo(Sw)_{output}$ ,  $Krow(Sw)_{output}$  at low water saturations. For this permeability ratio, end points are not significantly influenced by small-scale heterogeneity. Figure 5 illustrates the effect of the permeability ratio between layers. Both  $Krwo(Sw)_{output}$ ,  $Krow(Sw)_{output}$  are very different from  $Krwo(Sw)_{input}$ ,  $Krow(Sw)_{input}$ . Increasing permeability ratios result in increasingly large bias in  $Krwo(Sw)_{output}$ ,  $Krow(Sw)_{output}$  at low water saturations. For large permeability ratios, apparent end points are significantly influenced by small-scale heterogeneity, particularly at the remaining oil saturation.

It is concluded that unsteady-state flood is very sensitive to along-bedding heterogeneity of permeability. Clearly unsteady-state flow should be avoided when this type of heterogeneity is known or suspected.

#### SS flood, along-bedding flow, negligible capillary pressure

For steady state flow along the bedding, increasing permeability ratios between zones, up to 100, were input. The thickness of the high permeability layer was one third of the core thickness. Figure 6 illustrates the effect of the permeability ratio between layers.  $Krwo(Sw)_{output}$ ,  $Krow(Sw)_{output}$  and  $Krwo(Sw)_{input}$ ,  $Krow(Sw)_{input}$  are almost superimposed in the intermediate  $Sw$  range. The main discrepancy is between  $Krow(Sw)_{output}$  and  $Krow(Sw)_{input}$  for high water saturations. Increasing permeability ratios result in slightly increasing bias in  $Krow(Sw)_{output}$  in this  $Sw$  range. Increasing the fraction of high permeability layer was also tested for a permeability ratio between layers equal to 10. The effect was significant, but similar discrepancies were observed between input and output Kr curves. The comparison between Figures 5 and 6 shows that the steady-state flood is much more robust than unsteady-state when isoperms and flow direction are parallel. However, it should be noted that steady-state flow still leads to pessimistic output Kr curves, mainly after breakthrough, for both remaining oil saturation and fractional flow curves when along-bedding heterogeneity is ignored.

#### USS flood, across-bedding flow, negligible capillary pressure

For unsteady state flow across the bedding, increasing permeability ratios between zones, up to 100, were input. In all cases,  $Sorw_{output}$  is very close to the true value and

$Krwo(Sorw_{output})$  is slightly lower.  $Krwo(Sw)_{output}$ ,  $Krow(Sw)_{output}$  and  $Krwo(Sw)_{input}$ ,  $Krow(Sw)_{input}$  are almost superimposed, as shown in Figure 7. It is concluded that relative permeability curves obtained from unsteady-state flood are not dependent on across bedding heterogeneity of permeability when the capillary pressure is negligible.

#### SS flood, across-bedding flow, negligible capillary pressure

For these tests of steady state floods increasing permeability ratios between zones, up to 100, were input. In all cases  $Krwo(Sw)_{output}$ ,  $Krow(Sw)_{output}$  and  $Krwo(Sw)_{input}$ ,  $Krow(Sw)_{input}$  are almost superimposed as presented in Figure 8. It is concluded that relative permeability curves obtained from steady-state floods are not dependent on across bedding heterogeneity of permeability when capillary pressure is negligible.

#### **Conclusions and recommendations from the relative permeability comparisons:**

Four conclusions can be drawn from above results:

1. Along-bedding flow is the most risky situation. When isoperms are parallel to the core axis, any significant permeability contrast between layers would lead to erroneously pessimistic Kr curves if not accounted for during the coreflood interpretation. Unsteady-state waterfloods give unreliable results in this case. Steady-state waterflood is more robust but will not always provide reliable Kr curves in all cases.
2. Short, along-bedding core samples are often used for coreflood tests. Sample length ranges from 3 to 7 centimetres. Such samples might exacerbate errors due to permeability contrast between layers. Semi-variograms of local permeability built from probe permeameter measurements on outcrop analogues often show “horizontal” correlation lengths exceeding several tens of centimetres (Goggin, 1988; Dreyer, 1990). In other words, the likelihood of the existence of a sample spanning “high” permeability streak is very large in short, along-bedding core samples. Such artefacts might be responsible for the large scatter in Kr curves observed within some data sets.
3. Detection of permeability contrast between layers should be performed prior to any waterflood tests in along-bedding core samples.
4. Across-bedding flow is the less risky situation when capillary forces are negligible. Reliable relative permeability curves can be achieved using either steady-state or unsteady-state techniques.

## **INTERPRETATION OF WATERFLOOD EXPERIMENTS IN HETEROGENEOUS SAMPLES**

The above results show that along-bedding flow is more prone to interpretation errors than across-bedding flow for the determination of water/oil Kr curves. In some field cases, core

floods can only be performed on heterogeneous samples, as illustrated by Figures 1 and 2. In such cases, waterfloods should preferably be carried out across-bedding in order to minimise misinterpretation of experimental results, as shown above. In other cases, composite cores are built using samples cut along-bedding. Differences in individual plug permeability also result in the flow direction being perpendicular to isoperms. In the following only across-bedding flow will be considered. In corefloods performed at low rates, capillary forces might not be negligible compared to buoyancy and viscous forces. In such cases, any permeability contrast might result in saturation gradients within the core. These saturation gradients might be strong and can result in large bias in the determination of relative permeability curves. Multi-rate unsteady-state core waterfloods are simulated to decipher the respective effects of relative permeability and capillary pressure curves. The initial part of the water flood experiment is carried out at relatively low flow rates. Flood rates are increased stepwise. These steps lead to changes in the balance between viscous and capillary forces and increases in oil recovery. This is an advantage for the simultaneous determination of  $K_r$  and  $P_c$  curves. Finally, the last steps at high differential pressure ensure that the capillary end-effect has been minimised. In this work, there is no attempt to look for an optimum design of the waterflood tests, as far as cumulative throughput or test duration are concerned. A fixed period of injection was selected for each step to ensure that oil production versus time was stabilised.

Figure 9 shows two types of capillary pressure curves which represent weakly water-wet or weakly oil-wet rocks respectively. Input capillary pressure curves are assumed to be dependent on permeability for waterflood simulations as illustrated by Figure 9. Figure 10 illustrates typical oil production responses to multi-rate waterfloods when isoperms are perpendicular to the core axis. The homogeneous water-wet case does not show any production jump when the injection rate is increased. The heterogeneous water-wet case shows small amounts of additional oil production after each rate increase. The heterogeneous oil-wet case shows significant oil production increases at each increase in injection rate. The magnitude of this additional oil increase is obviously rate dependent. Even more interesting is the evolution of local  $S_w$  profiles in both cases, as illustrated by Figures 11 a and b. In the oil-wet case, oil is left behind in low permeability zones. In the water-wet case, oil is preferentially trapped in the high permeability zones as pointed out by Kortekaas (1985). Moreover, in the more water-wet case, increase in flooding rates shifts the water saturation from the positive to the negative branch of the capillary pressure curves to give saturation gradients that vary within zones. These figures highlight that local saturation profiles not only display end-effects but also describe the interplay between small-scale heterogeneity and wettability. Consequently, both oil production increases and changes in local  $S_w$  profiles with rate enable discrimination between capillary pressure and relative permeability effects on the waterflood response. It is then concluded that local  $S_w$  profiles are worth incorporating in the interpretation of waterfloods on heterogeneous cores.

Tests were carried out to evaluate whether Kr curves could be reliably obtained from an heterogeneous core when capillary forces are no longer negligible compared to gravity and viscous forces. The same approach was used to compare  $Krwo(Sw)_{output}$ ,  $Krow(Sw)_{output}$  and  $Krwo(Sw)_{input}$ ,  $Krow(Sw)_{input}$ . However  $Sw(x, t)$  are now considered as the “experimental observations” obtained during the waterflood in addition to  $Q_w(t)$ ,  $Q_o(t)$ ,  $D_p(t)$ . Two different wettability cases are also studied (i.e. weakly water-wet and weakly oil-wet). The same capillary pressure curves as shown in Figure 9 are used. For the inversion of waterflood results, it is assumed that wettability and local permeabilities are known from other sources of information

In the weakly water-wet case,  $Sorw_{output}$  is very close to the true value: 0.275 compared to 0.25, as is  $Krwo(Sorw_{output})$ : 0.232 compared to 0.25. The overall core values are very close to true values because the final  $Sw$  profiles are very flat, as shown by Figure 11a.  $Krwo(Sw)_{output}$ ,  $Krow(Sw)_{output}$  and  $Krwo(Sw)_{input}$ ,  $Krow(Sw)_{input}$  are very close. In the weakly oil-wet case,  $Sorw_{output}$  is further from the true value: 0.31 compared to 0.25, as is  $Krwo(Sorw_{output})$ : 0.18 compared to 0.25. The overall core value  $Sorw_{output}$  is not close to the true values because intermediate  $Sw$  profiles still show large saturation gradients within the core, as shown by Figure 11b. When the inversion is only constrained by overall  $Sorw_{output}$ , the agreement between  $Krwo(Sw)_{output}$ ,  $Krow(Sw)_{output}$  and  $Krwo(Sw)_{input}$ ,  $Krow(Sw)_{input}$  is not so good. A better agreement is obtained when the inversion is constrained by  $Sorw_{local}$ , which is chosen among the smallest  $Sorw$  observed on saturation profiles. Finally, there is a satisfactory agreement between  $Krwo(Sw)_{output}$ ,  $Krow(Sw)_{output}$  and  $Krwo(Sw)_{input}$ ,  $Krow(Sw)_{input}$  as illustrated by Figure 12, if both early and very late profiles are input. Errors bars on both  $Krwo(Sw)_{output}$ ,  $Krow(Sw)_{output}$  are large in the low  $Sw$  range, small in the medium and high  $Sw$  range and increase again very close to  $Sorw$ . The large confidence interval in the low  $Sw$  range is due to the lack of constraining “experimental” observations. In fact, this low  $Sw$  range is compressed within the front; in-situ  $Sw$  profiles do not provide valuable information, especially for the weakly oil-wet case. At the same time, pre-breakthrough liquid production does not provide any data about the ratio  $Krow/Krwo$ . However, this large confidence interval in the low  $Sw$  range has a limited impact on the reliability of relative permeability curves obtained by inversion of unsteady-state floods. In fact, the key point is the small confidence interval within the  $Sw$  range above the water saturation at the front. This ensures that the reservoir waterflood simulation will be correct. In such cases, the saturation gradients within the core are compressed by increased viscous forces. This is illustrated in Fig. 13 by in-situ experimental  $Sw$  profiles on an unconsolidated composite core made of 3 horizontal plugs. Increase in flooding rate results in the compression of the saturation gradient observed between core plugs A and B due to permeability differences.

### **Conclusions on the impact of capillary pressure:**

Reliable relative permeability curves can be obtained from across-bedding, unsteady-state flow when the samples are weakly water-wet or weakly oil-wet, provided that local permeabilities and in-situ saturation profiles are available and incorporated in the interpretation process.

### **DISCUSSION**

The above results are consistent with conclusions by Ferreol (1997): water/oil relative permeability curves were correctly extracted using production data and local saturation profiles coming from an unsteady-state waterflood on an intermediate wet, across-bedding sample. However, Ferreol used experimental design to perform the optimum selection of input parameters for numerical simulation, rather than inversion based on gradient estimates. This confirms that, whatever the mathematical method used to converge on the solution, reliable Kr curves can be estimated from an across-bedding sample, provided that multi-rate tests are carried out and that permeability as well as in-situ Sw profiles are measured and incorporated in the interpretation.

Although our conclusions appear to differ from those by Sylte (1998), there is no major contradiction. Sylte presented results on first drainage of water by oil. This type of displacement results in strong capillary end-effect because a non-wetting fluid is injected. Moreover any significant permeability variation along the core would result in large saturation gradients because drainage Pc curves are assumed to depend on permeability. Drainage is obviously an extreme case. On the other hand, our results show that reliable Kr curves can be extracted from heterogeneous cores when capillary forces are negligible, as small-scale heterogeneity does not generate strong saturation gradients along the core. This case is obviously closer to actual waterflood tests on weakly water-wet or weakly oil-wet rocks than drainage, particularly when flooding rate is increased stepwise.

Sylte obtained reliable estimates of Kr curves when permeability variations along the cores were input. This is consistent with our findings. Input of permeability zones in the direct waterflood simulation also allows prediction of saturation gradients within the core due to heterogeneity. Comparison between simulated and experimental Sw profiles ensures that both relative permeability and capillary pressure curves can be determined simultaneously.

### **REFERENCES**

- Corbett, P.W, Ringrose, P.S. : “ Laminated Clastic Reservoirs : The Interplay of Capillary Pressure and Sedimentary Architecture” SPE 24699, 1992.
- Corey, A.T., Rathjens, C.H. : “Effect of Stratification on Relative Permeability” Petroleum Transactions AIME, 1956.

- Dauba C., Hamon G. : “Stochastic description of experimental 3D permeability fields in vuggy reservoirs” SCA 9828, 1998, The Hague (Netherlands).
- Dauba C., Hamon G. : “Application of miscible displacements to identify along-axis heterogeneities on core flood samples” SCA 9934, 1999, Golden, Colorado, USA.
- Dreyer, D. ; Scheie, A. : “Mini-permeameter-based study of permeability Trends in Channel Sand bodies” AAPG bulletin, V74, n°4, April 1990.
- Ferreol, B.; Corre B.: “Determining Relative Permeabilities by Use of Experimental Design for very Heterogeneous Samples” ECMOR 97.
- Fincham, T. ; Gouth F. : “Improvements of coreflood design and interpretation using a new software” SCA 0029, Abu Dhabi, 2000.
- Goggin, D ; Chandler, M : “Patterns of permeability in eolian deposits : Page sandstone (Jurassic), Northeastern Arizona” SPEFE, June 1988.
- Hamon G. : “Oil water gravity drainage mechanisms in oil-wet fractured reservoirs” SPE 18366, Europec conference, London, 1988.
- Honarpour, M.M. ; Cullick, A.S. : “ Influence of Small-Scale Rock Laminations on Core Plug Oil/Water Relative Permeability and Capillary Pressure” SPE 27968, Tulsa, 1994.
- Honarpour, M.M. ; Cullick, A.S. : “Effect of Rock Heterogeneity on Relative Permeability : Implications for Scale-Up” SPE 29311, 1995.
- Huang, Y. ; Ringrose, P.; Sorbie, K.S.; Tudhope, S.W.: “Waterflood Displacement Mechanisms in a Laminated Rock Slab : Validation of Predicted Capillary Trapping Mechanisms” SPE 28942, 1994.
- A) Huang, Y. ; Ringrose, P. : “Experimental Determination of Residual and Remaining Oil in Laminated Rock Samples” 8eme Symposium Européen IOR, Vienne, Autriche, Mai 1995.
- B) Huang, Y. ; Ringrose, P. : “ The effects of Heterogeneity and Wettability on Oil Recovery from Laminated Sedimentary Structures” SPE 30781, 1995.
- Huppler, J.D. : “Waterflood Relative Permeability in Composite Cores” JPT Forum dans JPT, Mai 1969.
- Johnson, E.; Bossler, D.; Neumann V.: “Calculation of Relative Permeability from displacement Experiments” Trans. AIME, 1958.
- Jones, S.C. and Roszelle, W.O.: “Graphical Techniques for Determining Relative Permeability from Displacement Experiments,” J. Pet. Tech. (May 1978) 807-17.
- Kortekaas, T. : “Water/oil Displacement Characteristics in Crossbedded Reservoir Zones” SPEJ, Dec. 1985.
- Leverett, M.: “Capillary behaviour in porous solids” Trans. AIME, 1941.
- Nordtvedt, J.; Urkedal, H.: “The significance of violated assumptions on core analysis results” SCA 9931, 1999, Golden, Colorado, USA.
- Sylte, A.; Mannseth, T: “Relative Permeability and Capillary Pressure: Effects of rock heterogeneity” SCA 9808, 1998, The Hague, Netherlands.

## **ACKNOWLEDGEMENTS**

The authors thank Elf Exploration Production for permission to publish this study. Helpful discussions with T. Fincham of Elf Geoscience Research Center, and with F. Gouth, J. Barro are gratefully acknowledged.

Figure 1: Surface map of probe permeameter permeabilities on a sandstone reservoir sample

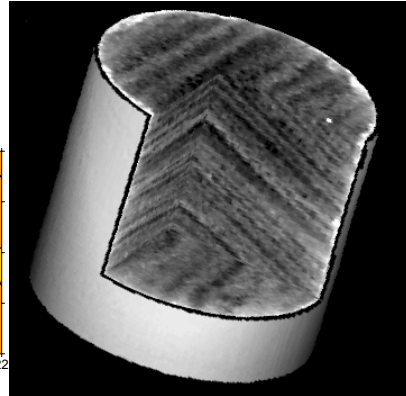
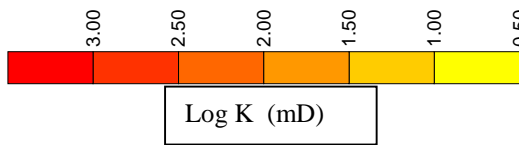
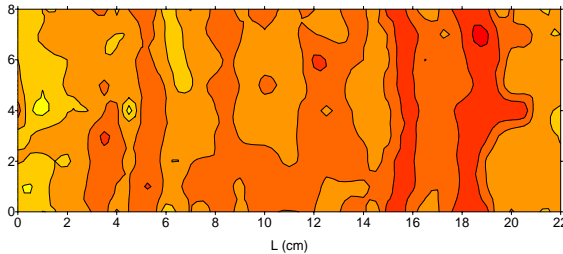


Figure 2: X-ray 3D image of a 5cm OD sandstone reservoir sample

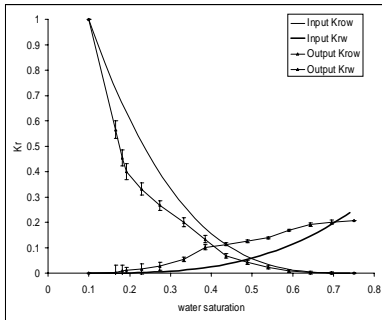


Figure 3: Errors bars in Krow, Krwo (output) resulting from the inversion process

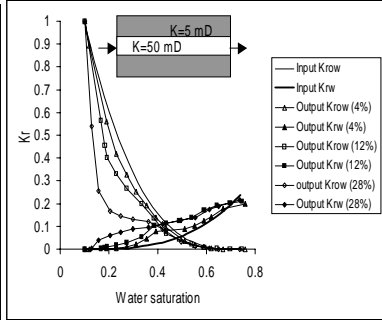


Figure 4: comparison between true and pseudo Kr curves (USS flood): effect of the fraction of high permeability layer

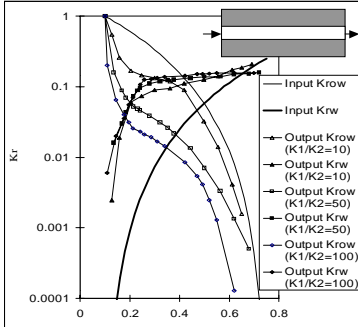


Figure 5: comparison between true and pseudo Kr curves (USS flood): effect of the permeability contrast between layers

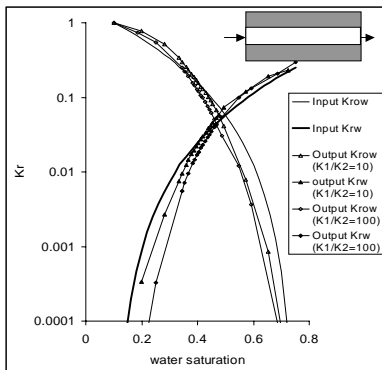


Figure 6: comparison between true and pseudo Kr curves (SS flood): effect of the permeability contrast between layers

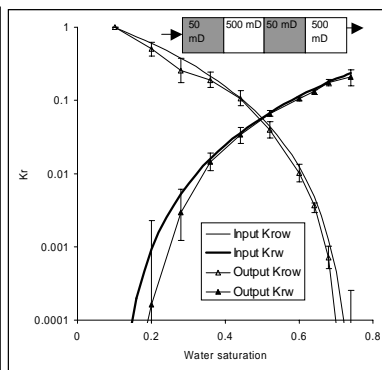


Figure 7: comparison between true and pseudo Kr curves (USS flood):

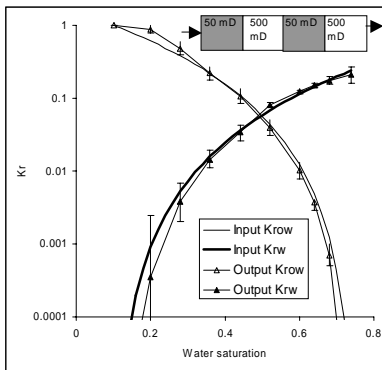


Figure 8: comparison between true and pseudo Kr curves (SS flood):

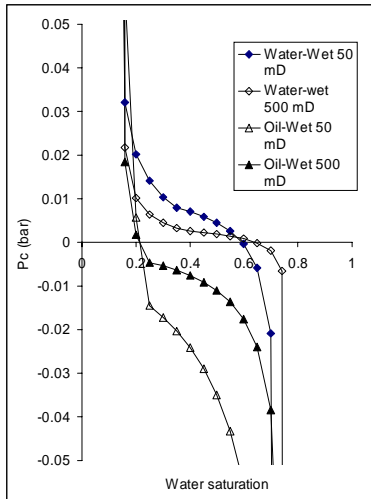


Figure 9 : Imbibition capillary pressure curves

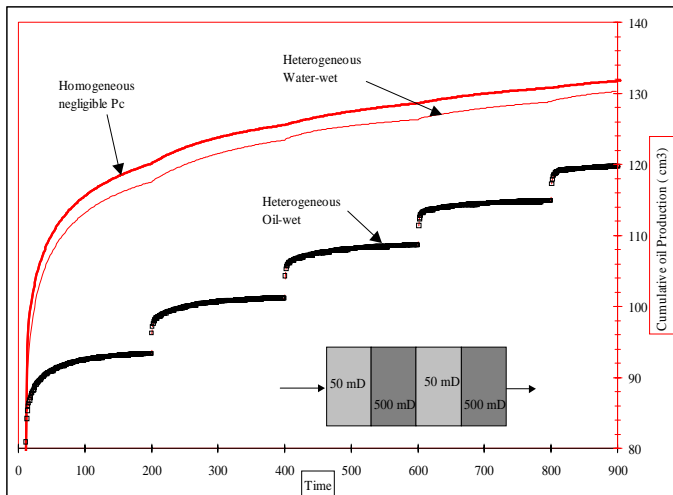


Figure 10 : Typical oil recovery response to multi-rate waterfloods

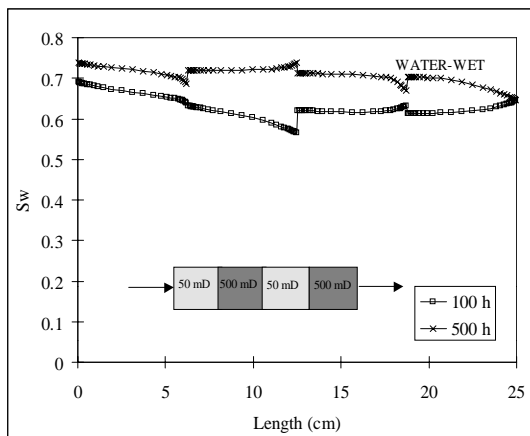


Figure 11a : Typical water saturation profile for an across-bedding, water-wet sample

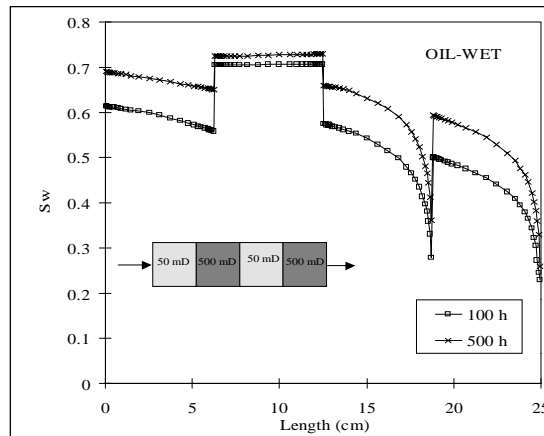


Figure 11b : Typical water saturation profile for an across-bedding, oil-wet sample

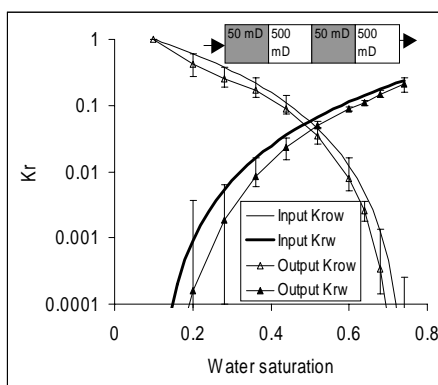


Figure 12 : comparison between true and estimated Kr curves (USS flood, weakly oil-wet case)

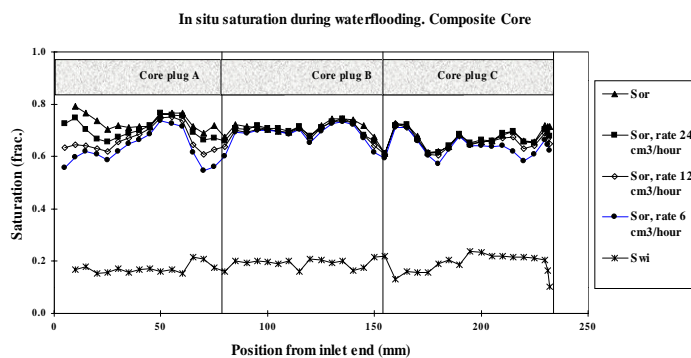


Figure 13 : permeability difference between core plugs A and B results in a saturation gradient. The flooding rate compresses this saturation gradient